Genetic variation of putative myokine signaling is dominated by biologic sex and sex hormones

Leandro M. Velez[1,2*], Cassandra Van[1,2*], Timothy M. Moore[3], Zhenqi Zhou[4], Casey Johnson[1,2], Andrea L. Hevener[4,5,6] and Marcus M. Seldin[1,2,6]

[1]Department of Biological Chemistry and [2]Center for Epigenetics and Metabolism, UC Irvine. Irvine, CA 92697, USA
[3]Department of Medicine, Division of Cardiology, David Geffen School of Medicine at UCLA, 675 Charles E. Young Dr., Los Angeles, CA 90095, USA
[4]Department of Medicine, Division of Endocrinology, Diabetes, and Hypertension, and [5]Iris Cantor-UCLA Women's Health Research Center, David Geffen School of Medicine at UCLA, 650 Charles E. Young Dr., Los Angeles, CA 90095, USA

*Authors contributed equally
[6]Co-corresponding authors

To whom correspondence should be addressed:
Marcus Seldin
UC Irvine Department of Biological Chemistry
314 Sprague Hall
Irvine, CA 92697
Phone: 949-824-6765
Email: mseldin@uci.edu

Impact Statement: Genetic architecture of muscle secreted protein functions are driven by sex

Keywords: Myokines, skeletal muscle, secreted proteins, endocrine physiology, population genetics, systems genetics.

Abstract

Skeletal muscle plays an integral role in coordinating physiologic homeostasis, where signaling to other tissues via myokines allows for coordination of complex processes. Here, we aimed to leverage natural genetic correlation structure of gene expression both within and across tissues to understand how muscle interacts with metabolic tissues. Specifically, we performed a survey of genetic correlations focused on myokine gene regulation, muscle cell composition, cross-tissue signaling and interactions with genetic sex in humans. While expression levels of a majority of myokines and cell proportions within skeletal muscle showed little relative differences between males and females, nearly all significant cross-tissue enrichments operated in a sex-specific or hormone-dependent fashion; in particular, with estradiol. These sex- and hormone-specific effects were consistent across key metabolic tissues: liver, pancreas, hypothalamus, intestine, heart, visceral and subcutaneous adipose tissue. To characterize the role of estradiol receptor signaling on myokine expression, we generated male and female mice which lack estrogen receptor α specifically in skeletal muscle (MERKO) and integrated with human data. These analyses highlighted potential mechanisms of sex-dependent myokine signaling conserved between species, such as myostatin enriched for divergent substrate utilization pathways between sexes. Several other putative sex-dependent mechanisms of myokine signaling were uncovered, such as muscle-derived *TNFA* enriched for stronger inflammatory signaling in females compared to males and *GPX3* as a male-specific link between glycolytic fiber abundance and hepatic inflammation. Collectively, we provide a population genetics framework for inferring muscle signaling to metabolic tissues in humans. We further highlight sex and estradiol receptor signaling as critical variables when assaying myokine functions and how changes in cell composition are predicted to impact other metabolic organs.

Introduction

Proteins secreted from skeletal muscle, termed myokines, allow muscle to impact systemic physiology and disease. Myokines play critical roles in a variety of processes, including metabolic homeostasis, exercise improvements, inflammation, cancer and cognitive functions[1–6]. Several notable examples include key peptide hormones such as myostatin and Interleukin-6 which exert potent actions in regulating autocrine/paracrine muscle physiology[7] and beneficial exercise-induced endocrine signaling[1], respectively. Despite the clear relevance of these factors in mediating a multitude of physiological outcomes, the genetic architecture, regulation and functions of myokines remains inadequately understood. Given that genetic sex contributes critically to nearly every physiologic outcome, it is essential to consider when relating specific mechanisms to complex genetic and metabolic interactions. Specifically, many metabolic traits impacted by myokines show striking sex differences arising from hormonal[8–11], genetic[8,12] or gene-by-sex interactions[13,14]. In this study, we leveraged natural genetic correlation structure of gene expression both within and across tissues to understand how muscle interacts with

metabolic tissues. Collectively, we provide a population genetics framework for inferring muscle signaling to metabolic tissues in humans. We further highlight sex and estradiol receptor signaling as critical variables when assaying myokine functions and how changes in cell composition are predicted to impact other metabolic organs.

Results

Sex hormone receptors are enriched with myokine expression independent of biological sex: Our goal was to exploit correlation structure of natural genetic variation to investigate how skeletal muscle communicates with and impacts metabolic organs. We first assayed regulation of myokines and changes in cellular composition, then related these observations to inferred cross-tissue signaling mechanisms (Fig 1A). Initially, we quantified differential expression of genes encoding all known secreted proteins (3,666 total) in skeletal muscle from 210 male and 100 female individuals[15]. While several notable myokines appeared different between sexes (Fig 1B), a striking majority of all secreted proteins (74%) showed no difference in expression between males and females (Fig 1C, Supplemental table 1). To understand potential sex-effects on the regulation of myokines, gene ontology enrichments were performed on genes which showed the strongest correlation with myokines corresponding to each category (male-specific, female-specific or non-sex specific). Here, the top 10 pathways which persisted in females were also always observed to overlap with the non-sex-specific category (Fig 1D). In contrast, pathways enriched for male-specific myokines were distinct (Fig 1D). Notably, the female and shared pathways suggested roles in epigenetics and RNA processing, while male-specific myokine coregulated processes were more enriched in metabolic pathways (ex. NADH metabolism) (Fig 1D). Further, a majority of myokines showed strong correlation with receptors mediating functions of androgens (androgen receptor -AR), estradiol (estrogen receptor α - ESR1), or both, regardless of sex-specific expression (Fig 1E). We note that expression of hormone receptors themselves were also not significantly different between sexes (Figure 1 - Figure supplement 1). To infer causality from hormone receptor regulation, we performed RNA-sequencing on mice lacking *Esr1* in skeletal muscle specifically (MERKO) and integrated these analyses with human myokine estimates. While myokines not regulated by *Esr1* showed little sex-specific differences in expression, those which were estrogen-dependent showed much stronger representation of sex-specificity, in particular in males (Fig 1F-G). Among these was the master regulator of skeletal muscle differentiation and proliferation, myostatin (MSTN), where hormone receptor correlations and gene expression were markedly higher in males compared to females (Fig 1H). Further, ablation of *Esr1* in mice uniquely drove expression changes in males (Fig 1H). These data suggest interactions between biologic sex and ESR1 to tightly regulate *MSTN* in males, where other factors could contribute more in females. Given that, like many bioactive secreted proteins, the regulation and sex-specificity of myostatin are additionally controlled via post-transcriptional mechanisms[16], we next explored gene expression changes at the protein level. Immunoblots were performed on skeletal muscle from male and female WT or MERKO mice (Figure 1- Figure supplement 2). Quantification of the processed form of myostatin showed that, consistent with the RNA-Seq in mice and humans, the protein trended toward higher levels in male compared to female mice, where ablation of *Esr1* showed a reduction (Fig 1I). Dissimilar to the mouse sequencing data but consistent with human correlations, female MERKO mice showed a reduction in processed form of myostatin relative to their WT controls (Fig 1I). Related to the sex-specific regulation of myostatin observed at both RNA and protein levels, gene expression also showed differences in functional annotations.

Here, the most highly enriched pathways in males showed GO terms related to glycolytic metabolism (Fig 1J) compared to oxidative phosphorylation in females (Fig 1K). These observations are consistent with previous studies which note myostatin-dependent increases in muscle mass in males, but not females[16,17], where estradiol signaling is suggested as a mechanism mediating these differences. These data demonstrate that, expression of most myokines are not different between genetic sexes; however, interactions between sex and hormone receptors likely play important roles in determining myokine regulation and local signaling.

Sex dominates cross-tissue pathways enriched for myokines – Given that expression levels of most myokines appeared similar between sexes, we next assessed putative functions across organs. We applied a statistical method developed to infer cross-tissue signaling which occur as a result of genetic variation[18–20]. Here, we assayed the distribution of midweight bicorrelation coefficients between myokine expression levels and global gene expression in key metabolic tissues including hypothalamus, heart, intestine, pancreas, liver, subcutaneous and visceral adipose tissue. Remarkably, nearly all highly significant correlations between myokines and target organ genes (putative direct interactions) showed sex-specific modes of operation (Fig 2A-H). This sex specificity also appeared more pronounced for positive correlations between myokines and target tissue genes, as compared to negative (Fig 2-H). Further, among these significant cross-tissue circuits, hormone receptor enrichments for these myokines was strongly dependent on the category (ex. significant only in females) rather than target tissue (Fig 2A-H). This observation further suggests that hormone receptor levels (ESR1 or AR) in muscle are a stronger determinant of myokine expression compared to genetic sex; however, sex is suggested to dominate coregulated signaling processes across organs via myokines. To gauge the relative impact of muscle steroid hormone receptors across organs, the number of significant correlations between *ESR1*, *AR* or both were quantified from muscle to each tissue. Here, *ESR1* showed an order of magnitude stronger enrichment across metabolic tissues compared to *AR* or correlation with both hormone receptors. (Fig 2I-J). Additionally, the number of significantly correlated cross-tissue male *ESR1* genes (Fig 2I) were three-fold higher than females (Fig 2J). Because both sex and ESR1 signaling appeared to contribute to the regulation and functions of myokines, significant cross-tissue enrichments were binned into categories taking into consideration whether myokines were driven by ESR1 in muscle, and/or showing a sex-specific mode of cross-organ significance. This analysis suggested that a majority of myokines were either driven by ESR1 and signaled robustly across sexes (Fig 2K, yellow) or signaled differently between sexes, but regulated independent of ESR1 (Fig 2K, red). These categories appeared to a much greater extent compared to a combination of both *ESR1*-driven myokine and sex-specific cross-tissue signaling (Fig 2K, beige) or neither (Fig 2K, seagreen). One notable example of predicted sex-specific signaling was observed for tumor necrosis factor alpha (TNFA). When compared between sexes, muscle *TNFA* showed markedly different putative target tissues (Fig 2L, left), as well as underlying functional pathways (Fig 2L, right). For example, overall inflammatory processes engaged by TNFA were stronger in adipose tissue in females; however, the same pathways were higher in liver and hypothalamus in males (Fig 2L, left). Collectively, these data show that genetic sex and related sex steroid hormones, particularly estradiol, exert dominant roles in regulating predicted tissue and pathway engagement by myokines.

Muscle cell proportions are similar between sexes, but associated changes across tissues show sex-specificity – To determine the potential impact of muscle composition on other tissues, we next surveyed muscle cellular proportions in the context of genetics and sex. Single-cell sequencing of human skeletal muscle[21] were integrated using cellular deconvolution[22] to estimate cellular composition in the population (Fig 3A). Here, a proportions in admixture approach[23] outperformed other methods (Figure 3 - Figure supplement 1) to capture a majority of established cell populations across individuals (Supplemental Table 2). Similar to myokine expression, no notable differences were observed between sexes in terms of cell composition, with the exception of modest higher glycolytic fiber in males, compared to elevated oxidative fiber levels in females (Fig 3B). Additionally, no differences were observed in the correlations within muscle between compositions (Figure 3 - Figure supplement 2); however, nearly every cross-tissue enrichment corresponding to an individual muscle cell type differed between sexes (Fig 3C). Generally, differences in skeletal muscle cell abundance was associated with changes in liver and visceral adipose tissue pathways in males, compared to pancreas in females (Fig 3C). In contrast to general myokine enrichments, cell proportions showed stronger correlations with *AR* when compared to *ESR1* across both sexes where the most abundant cell types were significantly enriched for both steroid hormone receptors (Fig 3D). To uncover potential direct mechanisms linking changes in cell composition to peripheral tissues, we correlated all myokines with cell composition profiles. Again, despite few differences between sexes in terms of myokine expression and cell composition, specific myokines highly correlating with individual cell type were markedly different between males and females with the exception of one, *APOD* in slow-twitch fibers (Fig 3E). To determine if variation in cell compositions corresponding to sex-specific tissue signaling via myokines was predicted to be likely, we implemented adjusted regression mediation analyses[24] for glycolytic fiber composition. Because male glycolytic fiber type abundance was selectively enriched for liver pathways such as immune cell activation and regulated exocytosis (Fig 3F), the top-genes driving these enrichments were used for mediation. The top-correlated muscle secreted protein with male glycolytic fiber type levels was secreted glutathione peroxidase 3 (GPX3). Here, adjusting regressions between glycolytic fiber and liver pathways on *GPX3* reduced the overall significance across tissues (Fig 3G), suggesting GPX3 as a potential mediator of this communication. These data point to a potential mechanism whereby muscle fiber abundance could buffer free radical generation in the liver, thereby feeding back on inflammation. This analysis appeared additionally sensitive to inferring non-dependent relationships between muscle cell types, top-ranked myokines and cross-tissue processes. For example, female glycolytic fibers were strongly enriched for pancreatic protein synthesis pathways; however, when adjusted for the top-ranked myokine *CES4A*, no changes in regression significance were observed (Fig 3F-G). These analyses suggest that male GPX3 is a potential mechanism whereby fast-twitch muscle signals to liver; however, the same cell type in females drive pancreas protein synthesis independent of CES4A. In summary, we show that cell composition is strongly conserved between sexes, but putative cross-tissue signaling of altered composition differs entirely. We further suggest putative myokines and mechanisms, as well as highlight the key regulatory roles of estrodiol in both sexes.

Discussion

Here we provide a population survey of skeletal muscle myokine regulation and putative functions using genetic variation and multi-tissue gene expression data. We find that in general, expression of myokines do not significantly differ between sexes; however, inferred signaling

mechanisms across tissues using regressions show strong sex specificity. Steroid hormone receptors, in particular *ESR1*, is highlighted as a key regulator of myokines and potentially interacting with biologic sex for proteins such as myostatin. Further integration with loss-of-function mouse models of *Esr1* highlighted the key roles of estradiol signaling in muscle in terms of myokine regulation and signaling across both sexes. Generation of pseudo-single-cell maps of muscle composition showed that, like myokines, muscle proportions are conserved between sexes, but inferred interorgan consequences differ substantially. When interpreting these findings, several considerations should be taken. While inter-tissue regression analyses have been informative to dissect mechanisms of endocrinology[18–20,25], observations can be subjected to spurious or latent relationships in the data. While causality for inter-organ signaling can be inferred statistically using approaches such as mediation as in Fig 3H, the only methods to provide definitive validation for new mechanisms is in experimental settings. Further, our current analyses rely on gene expression to guide functions of proteins which are typically strongly regulated by post-transcriptional processes. As shown for myostatin (Fig 1), gene expression analyses can miss key functional aspects of proteins, where follow-up studies and resources focused on protein and subsequent modification levels could heavily improve predictions. In addition, we anticipate that estimates for ESR1 effects on myokines in this study likely represents an underestimated number of all human ESR1-driven myokines. One limitation here includes that annotation of known orthologous mouse-human genes[26] remains somewhat limited. Furthermore, cell composition estimates from single-cell sequencing data are inferred from gene expression, where histological or flow cytometry-based methods can provide much more accurate direct quantifications. Clearly, morphological and structural differences between sexes have been observed in humans[27] which, if not apparent in gene expression, would be missed in this analysis. Future studies addressing these points will help to clarify context- and mechanism-relevant muscle-derived endocrine communication axes. In summary, this study highlights the key contributions of sex and sex steroid hormones in mediating myokine functions.

Material and methods

All datasets used, R scripts implemented for analyses and detailed walkthrough guide is available via: https://github.com/Leandromvelez/myokine-signaling

Key Resource Table:

Reagent type	Designation	Source or reference	Identifiers	Additional information
Antibody	anti-MSTN (Goat polyclonal)	R&D	AF788	(1:1000)
Antibody	Rabbit anti-Bactin (Rabbit polyclonal)	Genetex	GTX109639	(1:1000)

Animals – All mice used in this study were approved by the University of California Los Angeles (UCLA) Animal Care and Use Committee, in accordance with Public Health Service guidelines with reference #92-169.

Data sources and availability – All data used in this study can be immediately accessed via github to facilitate analysis. Human skeletal muscle and metabolic tissue data was accessed through GTEx V8 downloads portal on August 18, 2021 and previously described[15]. To enable sufficient integration and cross-tissue analyses, these data were filtered to retain genes which were detected across tissues where individuals were required to show counts > 0 in 1.2e6 gene-tissue combinations across all data. Given that our goal was to look across tissues at enrichments, this was done to limit spurious influence of genes only expressed in specific tissues in specific individuals. Post-filtering consists of 310 individuals and 1.8e7 gene-tissue combinations. Single-cell sequencing from skeletal muscle used for deconvolution was obtained from[21]. *Esr1* WT and KO mouse differential expression results are available on Github as well, where raw sequencing data has been deposited in NIH sequence read archive (SRA) under the project accession: PRJNA785746

Selection of secreted proteins – To determine which genes encode proteins known to be secreted as myokines, gene lists were accessed from the Universal Protein Resource which has compiled literature annotations terms for secretion[28]. Specifically, the query terms to access these lists were: locations:(location:"Secreted [SL-0243]" type:component) AND organism:"Homo sapiens (Human) [9606]" where 3666 total entries were found.

Differential expression of myokines dependent on sex – Gene expression counts matrices were isolated from the rest of the tissues, where individual genes were retained if the total number of counts exceeded 10 in 50 individuals. Next, only genes encoding secreted proteins (above) were retained, where logistic regression contrasted on sex was performed using DESeq2. Differential expression summary statistics were used for downstream binning of sex-specificity based on an empirical logistic regression pvalue <0.05. This threshold was used to reflect a least stringent cutoff where, despite potential false positive influence, genes which nominally trended toward sex-specific expression could be included in those categories. Given that the general conclusions supported very few proportions of myokines showing sex-specific patterns of expression, this conclusion would only be further exaggerated if the DE threshold were made more stringent and lessened the number of myokines in each category.

Regression analyses across tissues – Regression coefficients and corresponding p-values across tissues were generated using WGCNA bicorandpvalue() function[23]. Myokine-target gene pairs were considered significant (ex. Fig 2A-H) at a threshold of abs(bicor) > 2 standard deviations beyond the average coefficient for the given target tissue of interest. In previous studies, this threshold of 2 standard deviations reflects adaptive permutation testing pvalues <0.01[18,19]. For analyses estimating cumulative patterns of concordance across tissues (ex. Fig 2I-L), empirical regression pvalues (students pvalue from bicor coefficients) of 0.01 (corresponding to abs(bicor)>0.1) were used to assay global patterns. While empirical pvalues are subjected to false positives, including these enables broad visualization of both potential direct interactions (ex. myokine-target gene) as well as coregulated processes across organs. It is important to note that we exclusively rely on these empirical pvalues when surveying broad correlation structures, whereas much more stringent and appropriate thresholds (ex. p<1e-6 for Fig 3G) were applied when inferring direct interactions.

Pathway enrichment analyses - For Fig 1I and Fig 3G, genes corresponding to pvalue cutoffs were visualized using Webgestalt[29] to enable streamline analysis. This tool enabled simultaneous overrepresentation testing of GO:BP (non-redundant), KEGG and Panther databases. For Fig. 1D, the top 1000 (by regression p-value) significant genes from myokines to all muscle bicorrelation analysis in females, males or non-sex specific datasets were assessed for enrichment in GO Biological Process terms using ClusterProfiler ver. 4.0.2 in R[30]. The resulting top ten GO terms in each dataset were integrated and plotted against the relative proportion of the p.adjusted value and visualized in the same graph using ggplot2.

Deconvolution of skeletal muscle – Raw single-cell RNA sequencing from skeletal muscle was obtained from[21]. These raw counts were analyzed in Seurat where cluster analyses identified variable cell compositions. Cell type annotations were assigned based on the top 30 genes (Supplemental table 2) assigned to each UMAP cluster through manual inspection and ENRICHR[31]. Finally, a normalized matrix of gene:cells was exported from Seurat and used to run deconvolution on skeletal muscle bulk sequencing. Using the ADAPTS pipeline[22], three deconvolution methods (nnls, dcq or proportions in admixture) were compared based on ability to robustly capture cell proportions (Figure 3 – supplemental figure 1), where proportion in admixture showed the best performance and subsequently applied to bulk sequencing.

ESR1 muscle KO generation, RNA-Seq and integration with human data – Muscle-specific Esr1 deletion was generated and characterized as previously described[11]. Whole quadriceps was pulverized at the temperature of liquid nitrogen. Tissue was homogenized in Trizol (Invitrogen, Carlsbad, CA, USA), RNA was isolated using the RNeasy Isolation Kit (Qiagen, Hilden, Germany), and then tested for concentration and quality with samples where RIN > 7.0 used in downstream applications. Libraries were prepared using KAPA mRNA HyperPrep Kits and KAPA Dual Index Adapters (Roche, Basel, Switzerland) per manufacturer's instructions. A total of 800-1000 ng of RNA was used for library preparation with settings 200-300 bp and 12 PCR cycles. The resultant libraries were tested for quality. Individual libraries were pooled and sequenced using a HiSeq 3000 at the UCLA Technology Center for Genomics and Bioinformatics (TCGB) following in house established protocols. Raw RNAseq reads were inspected for quality using FastQC v0.11.9 (Barbraham Institute, Barbraham, England). Reads were aligned and counted using the Rsubread v2.0.0[32] package in R v3.6 against the Ensembl mouse transcriptome (v97) to obtain counts. Lowly expressed genes (>80% samples with 0 counts for particular gene) were removed. Samples were analyzed for differential expression using DeSeq2 v1.28.0[33].

Conservation of gene between mice and humans - To find which myokines and pathways were conserved between mice and humans, all orthologous genes were accessed from MGI vertebrate homology datasets, which have been compiled from the Alliance for Genome Resources[26] and intersected at the gene level (roughly 18,000 genes).

Immunoblotting procedures - Muscle tissue was homogenized in the TissueLyser II (Qiagen) at 4 °C in RIPA lysis buffer supplemented with protease inhibitors. The homogenate was centrifuged at 4 °C for 10 min at 10 000 g, and the protein concentrations in the supernatant were measured by the BCA assay (Bio-Rad). After boiling protein samples for 5 min, 20 µg of protein

from each sample were applied on an SDS–polyacrylamide gel (10%) and electrophoresis was performed at 100 V for 1.5 h. The separated proteins were transferred to nitrocellulose membranes and membranes were blocked for 1.5 h in TBS (4 mM Tris–HCl, pH 7.5, and 100 mM NaCl) containing 5% skim milk plus Tween 20, at room temperature. Goat polyclonal anti-GDF8 (Myostatin) (R&D, catalog number AF788) at 1/1000 dilution were applied overnight as primary antibody. After washings, membranes were incubated with Goat IgG HRP-conjugated Antibody (R&D HAF017) at 1/10000 for 2 h, and bound HRP activity was detected with an enhanced chemiluminescence method (Clarity Western ECL, BioRad), by means of a chemilumiscence detection system (ChemiDoc System, BioRad). The intensities of the resulting bands were quantified by densitometry (ImageJ free software). Membranes were immersed in a stripping solution for 10 mins (Restore PLUS Western Blot, Thermo Fisher), and then the process repeated with a rabbit polyclonal anti-beta actin (GeneTex GTX109639) at 1/1000 dilution as loading control to assess uniformity of loading.

Acknowledgements

We acknowledge the following funding sources for supporting these studies: LMV, CV, CJ and MMS were supported by NIH grants HL138193, DK130640 and DK097771. ZZ was supported by NIH grant DK125354. T.M.M. was supported by the UCLA Intercampus Medical Genetics Training Program (T32GM008243). ALH is supported by NIH grants U54 DK120342, R01 DK109724, and P30 DK063491.

Conflict of interest

The authors have no conflicts of interest to declare

References

1. Severinsen, M. C. K. & Pedersen, B. K. Muscle–Organ Crosstalk: The Emerging Roles of Myokines. *Endocrine Reviews* **41**, 594–609 (2020).
2. Eckel, J. Myokines in metabolic homeostasis and diabetes. *Diabetologia* **62**, 1523–1528 (2019).
3. Febbraio, M. A. & Pedersen, B. K. Who would have thought — myokines two decades on. *Nat Rev Endocrinol* **16**, 619–620 (2020).
4. Kim, S. *et al.* Roles of myokines in exercise-induced improvement of neuropsychiatric function. *Pflugers Arch - Eur J Physiol* **471**, 491–505 (2019).

5. Kim, J.-S., Galvão, D. A., Newton, R. U., Gray, E. & Taaffe, D. R. Exercise-induced myokines and their effect on prostate cancer. *Nat Rev Urol* **18**, 519–542 (2021).
6. Seldin, M. M. & Wong, G. W. Regulation of tissue crosstalk by skeletal muscle-derived myonectin and other myokines. *Adipocyte* **1**, 200–202 (2012).
7. Kollias, H. D. & McDermott, J. C. Transforming growth factor-β and myostatin signaling in skeletal muscle. *Journal of Applied Physiology* **104**, 579–587 (2008).
8. Mauvais-Jarvis, F., Arnold, A. P. & Reue, K. A Guide for the Design of Pre-clinical Studies on Sex Differences in Metabolism. *Cell Metab* **25**, 1216–1230 (2017).
9. Mauvais-Jarvis, F. Sex differences in metabolic homeostasis, diabetes, and obesity. *Biol Sex Differ* **6**, 14 (2015).
10. Clegg, D. J. & Mauvais-Jarvis, F. An integrated view of sex differences in metabolic physiology and disease. *Molecular Metabolism* **15**, 1–2 (2018).
11. Ribas, V. *et al.* Skeletal muscle action of estrogen receptor α is critical for the maintenance of mitochondrial function and metabolic homeostasis in females. *Sci Transl Med* **8**, 334ra54 (2016).
12. Zore, T., Palafox, M. & Reue, K. Sex differences in obesity, lipid metabolism, and inflammation-A role for the sex chromosomes? *Mol Metab* **15**, 35–44 (2018).
13. Norheim, F. *et al.* Gene-by-Sex Interactions in Mitochondrial Functions and Cardio-Metabolic Traits. *Cell Metab.* **29**, 932-949.e4 (2019).
14. Chella Krishnan, K. *et al.* Sex-specific genetic regulation of adipose mitochondria and metabolic syndrome by Ndufv2. *Nat Metab* (2021) doi:10.1038/s42255-021-00481-w.
15. GTEx Consortium *et al.* Genetic effects on gene expression across human tissues. *Nature* **550**, 204–213 (2017).

16. McMahon, C. D. *et al.* Sexual dimorphism is associated with decreased expression of processed myostatin in males. *Am J Physiol Endocrinol Metab* **284**, E377-381 (2003).
17. Reisz-Porszasz, S. *et al.* Lower skeletal muscle mass in male transgenic mice with muscle-specific overexpression of myostatin. *Am J Physiol Endocrinol Metab* **285**, E876-888 (2003).
18. Seldin, M. M. *et al.* A Strategy for Discovery of Endocrine Interactions with Application to Whole-Body Metabolism. *Cell Metab.* **27**, 1138-1155.e6 (2018).
19. Seldin, M. M. & Lusis, A. J. Systems-based approaches for investigation of inter-tissue communication. *J. Lipid Res.* **60**, 450–455 (2019).
20. Seldin, M., Yang, X. & Lusis, A. J. Systems genetics applications in metabolism research. *Nat Metab* **1**, 1038–1050 (2019).
21. Rubenstein, A. B. *et al.* Single-cell transcriptional profiles in human skeletal muscle. *Sci Rep* **10**, 229 (2020).
22. Danziger, S. A. *et al.* ADAPTS: Automated deconvolution augmentation of profiles for tissue specific cells. *PLoS ONE* **14**, e0224693 (2019).
23. Langfelder, P. & Horvath, S. WGCNA: an R package for weighted correlation network analysis. *BMC Bioinformatics* **9**, 559 (2008).
24. Yokota, T. *et al.* Type V Collagen in Scar Tissue Regulates the Size of Scar after Heart Injury. *Cell* (2020) doi:10.1016/j.cell.2020.06.030.
25. Li, H. & Auwerx, J. Mouse Systems Genetics as a Prelude to Precision Medicine. *Trends Genet* **36**, 259–272 (2020).
26. Alliance of Genome Resources Consortium. Alliance of Genome Resources Portal: unified model organism research platform. *Nucleic Acids Res* **48**, D650–D658 (2020).

27. Haizlip, K. M., Harrison, B. C. & Leinwand, L. A. Sex-based differences in skeletal muscle kinetics and fiber-type composition. *Physiology (Bethesda)* **30**, 30–39 (2015).
28. The UniProt Consortium *et al.* UniProt: the universal protein knowledgebase in 2021. *Nucleic Acids Research* **49**, D480–D489 (2021).
29. Liao, Y., Wang, J., Jaehnig, E. J., Shi, Z. & Zhang, B. WebGestalt 2019: gene set analysis toolkit with revamped UIs and APIs. *Nucleic Acids Res* **47**, W199–W205 (2019).
30. Wu, T. *et al.* clusterProfiler 4.0: A universal enrichment tool for interpreting omics data. *The Innovation* **2**, 100141 (2021).
31. Kuleshov, M. V. *et al.* Enrichr: a comprehensive gene set enrichment analysis web server 2016 update. *Nucleic Acids Res* **44**, W90-97 (2016).
32. Liao, Y., Smyth, G. K. & Shi, W. The R package Rsubread is easier, faster, cheaper and better for alignment and quantification of RNA sequencing reads. *Nucleic Acids Research* **47**, e47–e47 (2019).
33. Love, M. I., Huber, W. & Anders, S. Moderated estimation of fold change and dispersion for RNA-seq data with DESeq2. *Genome Biol* **15**, 550 (2014).

Figure Legends

Figure 1. Sex and hormone effects on myokine regulation. A, overall study design for integration of gene expression from muscle from 310 humans, single-cell RNA-seq, muscle-specific deletion of *Esr1* to infer interorgan coregulatory process across major metabolic tissues. B-C, Differential expression analysis for sex was performed on all genes corresponding to secreted proteins in skeletal muscle (Myokines). The specific genes which showed significant changes in each sex are shown as a volcano plot (B) and the relative proportions of myokines corresponding to each category at a least-stringent logistic regression p-value less than 0.05 (C). D, for each differential expression category based on sex shown in C, myokines were correlated with all other muscle genes for pathway enrichment. Then the top 10 enriched pathways in males, females, or non-sex specific (by overall significance) were visualized together where number of genes corresponding to each category shown as a relative proportion. E, the same analysis as in D, except instead of myokines being correlated with *AR, ESR1*, both hormone receptors, or neither, as compared to correlating with all genes. F-G, Myokines were binned into

2 categories based on significant differential expression(logistic regression adjusted p-value<0.05) between muscle-specific WT and MERKO mice (F) or those that showed no change (G), then visualized as relative proportions within each category shown in C. H, Midweight bicorrelation (bicor) coefficients (color scheme) and corresponding regression p-values (filled text) are shown for muscle *MSTN* ~ *ESR1* or *AR* in both sexes (top). Below, correlations are shown for differential expression log2FC (color scheme) and corresponding logistic regression p-values (text fill) for *MSTN* between sexes in humans or WT vs MERKO mice. I, Quantification of processed form of myostatin (Figure 1 – figure supplement 2 bottom band) relative to beta-actin in WT or MERKO muscle in male or female mice. Pvalues calculated using a students t-test. J-K, the top 3 pathways of genes which significantly (p<1e-4) correlated with muscle *MSTN* in males (J) or females (K). For human data, n=210 males and n=100 females. For mouse MERKO vs WT comparisons, n=3mice per group per sex. p-values from midweight bicorrelations were calculated using the students p-value from WGCNA and logistic regression p-values were calculated using DESeq2.

Figure 1: Figure supplement 1 **- Skeletal muscle sex hormone receptor expression between sexes:** Normalized gene expression levels for androgen receptor (AR) or estrogen receptor (ESR1) (y-axis) in each sex (x-axis). None of the expression levels were significantly different between sexes (students t-test)

Figure 1: Figure Supplement 2 **- Immunoblot for myostatin in EDL muscle from WT and MERKO male and female mice.** Full Immunoblots shown for skeletal muscle lysate blotted for myostatin (top) or β-actin (bottom) corresponding to different C57BL/6J male (left) or female (right) mice in either WT (floxed) or KO (floxed-cre) for skeletal muscle *Esr1*. Band sizes shown to indicate either precursor (top band) or processed/LAP form (bottom band) of myostatin.

Figure 2. Sex and hormone effects on myokine regulation. A-H, Key illustrating analysis for distribution of midweight bicorrelation coefficients between all myokines in skeletal muscle and global transcriptome measures in each target tissue. Coefficients are plotted between sexes (left), where proportions for 2SD > mean are subdivided into occurrence uniquely in females, males, or shared (middle). The significant (2SD >mean) myokines identified in each category were then binned into hormone receptor correlations for *ESR1, AR,* both or neither (right). This analysis was performed on all myokines across subcutaneous adipose tissue (B), visceral adipose (C), heart (D), hypothalamus (E), small intestine (F), liver (G) and pancreas (H). I-J, Significant cross-tissue correlations between muscle *ESR1, AR,* or both hormone receptors are colored by tissue and shown for males (I) or females (J). K, For each tissue (y-axis), the ratio of significant cross-tissue correlations per muscle myokine (x-axis) are shown and colored by categories of: either the myokine regulated by *ESR1* and/or a significant target tissue regression occurring specifically in one sex. L, Number of significant cross-tissue correlations with muscle *TNFα* are shown for each sex and colored by tissue as in I-L (left). The -log10(p-value) of significance in an overrepresentation test (x-axis) are shown for top significant inter-tissue pathways for muscle TNFα in each sex (right).

Figure 3. Genetic variation of muscle cell proportions and coregulated cross-tissue processes. A, Uniform Manifold Approximation and Projection (UMAP) for skeletal muscle single-cell sequencing used to deconvolute proportions. B, Mean relative proportions of pseudo-

single-cell muscle cell compositions (denoted by color) between sexes. C, Number of significant cross-tissue correlations (y-axis) corresponding to each skeletal muscle type in each sex (x-axis). Target tissues are distinguished by color, where NS (male platelets) denotes that no significant cross-tissue correlations were observed. D, Heatmap showing significance of correlations between skeletal muscle hormone receptors and cell proportions, * = p<0.01. E, the strongest enriched myokines are plotted for each myokine (y-axis, -log10p-value of myokine ~ cell composition) are shown for each muscle proportion for each sex (x-axis). Gene symbols for myokines are shown above each line, where red lines indicate positive correlations between myokine and cell type and blue shows inverse relationships. F, Significant cross-tissue correlated genes in liver (blue) and pancreas (purple) for muscle fast twitch glycolytic fibers (P<1e-6) were used for overrepresentation tests where enrichment ratio of significance (x-axis) is shown for each pathway and sex (y-axis). G, Heatmap showing the regression significance of the top 5 genes corresponding to inflammation (liver), exocytosis (liver) and protein synthesis (pancreas) for proportions of fast-twitch fiber type (un-adj). Below each correlation between fast-twitch fiber and liver or pancreas gene, the same regressions were performed while adjusting for abundance of select myokines in each sex. *=p<1e-6.

***Figure 3: Figure supplement 1*- Comparisons of deconvolution methods:** Cell proportions were estimated from skeletal muscle sequencing across the 310 individuals in GTEx. Here, comparisons of the three most common methods (DCQ, NNLS and porportionsInAdmixture) were plotted for each pseudo-sc-proportion, where proportionsInAdmixture method captured the largest relative number of cell types

***Figure 3: Figure supplement 2* - Cell composition correlations within each sex:** Heatmaps showing regressions for cell proportions in males (left) or females (right), * = regression pvalue<0.01

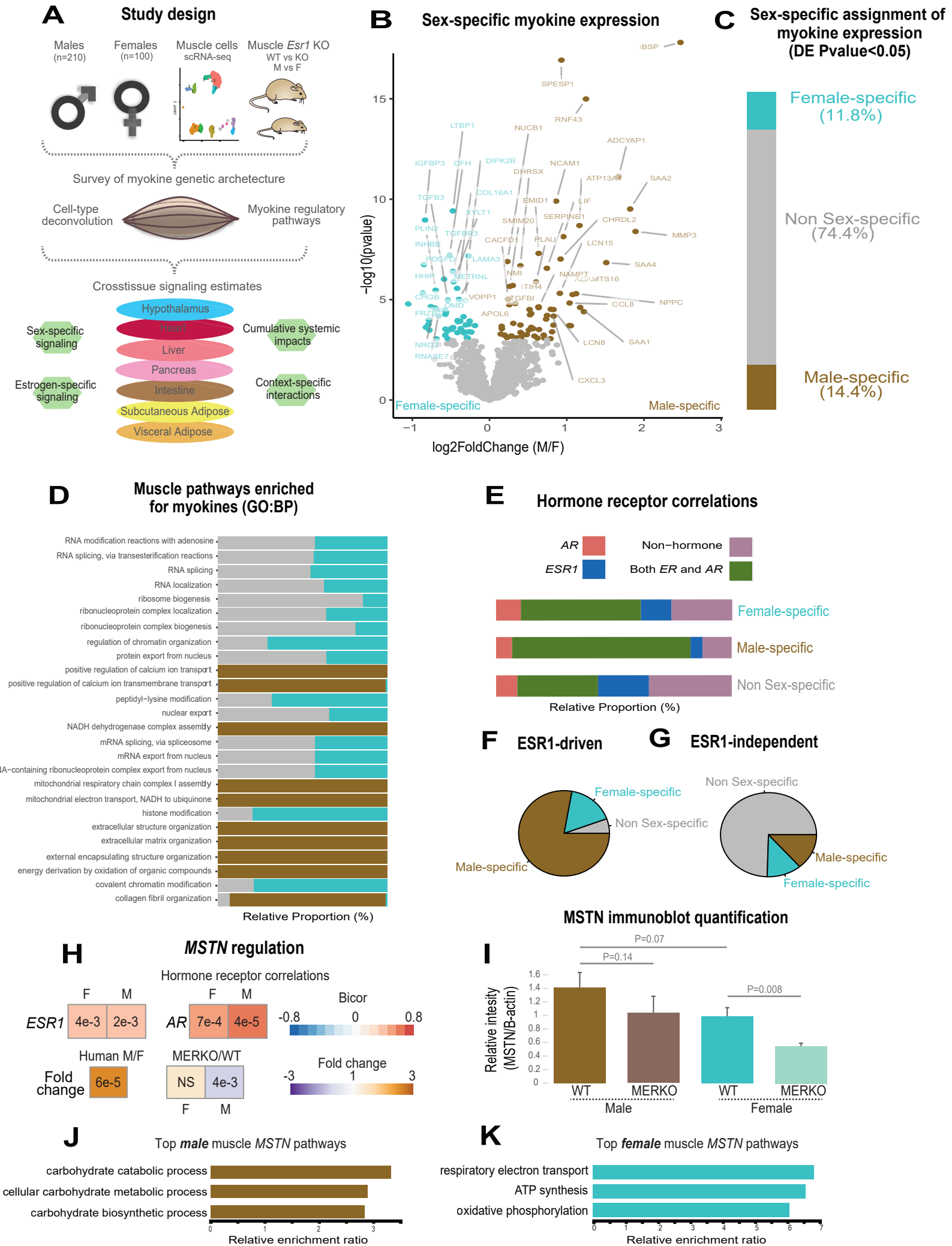
A
Study design
Males (n=210)
Females (n=100)
Muscle cells scRNA-seq
Muscle Esr1 KO WT vs KO M vs F
Survey of myokine genetic archetecture
Cell-type deconvolution
Myokine regulatory pathways
Crosstissue signaling estimates
Hypothalamus
Heart
Liver
Pancreas
Intestine
Subcutaneous Adipose
Visceral Adipose
Sex-specific signaling
Estrogen-specific signaling
Cumulative systemic impacts
Context-specific interactions
B
Sex-specific myokine expression
−log10(pvalue)
log2FoldChange (M/F)
Female-specific
Male-specific
IBSP
SPESP1
RNF43
LTBP1
NUCB1
ADCYAP1
IGFBP3
CFH
DIPK2B
NCAM1
DHRSX
ATP13A4
SAA2
TGFB3
COL16A1
EMID1
LIF
XYLT1
SERPINE1
CHRDL2
PLIN2
SMIM20
TGFBR3
CACFD1
PLAU
LCN15
MMP3
INHBB
PDGFD
LAMA3
SAA4
HHIP
METRNL
NMI
NAMPT
ADAMTS16
ITIH4
CHGB
VOPP1
TGFBI
CCL8
NPPC
FRZB
OMD
APOL6
LCN8
SAA1
NRG2
RNASE7
CXCL3
C
Sex-specific assignment of myokine expression (DE Pvalue<0.05)
Female-specific (11.8%)
Non Sex-specific (74.4%)
Male-specific (14.4%)
D
Muscle pathways enriched for myokines (GO:BP)
RNA modification reactions with adenosine
RNA splicing, via transesterification reactions
RNA splicing
RNA localization
ribosome biogenesis
ribonucleoprotein complex localization
ribonucleoprotein complex biogenesis
regulation of chromatin organization
protein export from nucleus
positive regulation of calcium ion transport
positive regulation of calcium ion transmembrane transport
peptidyl−lysine modification
nuclear export
NADH dehydrogenase complex assembly
mRNA splicing, via spliceosome
mRNA export from nucleus
mRNA−containing ribonucleoprotein complex export from nucleus
mitochondrial respiratory chain complex I assembly
mitochondrial electron transport, NADH to ubiquinone
histone modification
extracellular structure organization
extracellular matrix organization
external encapsulating structure organization
energy derivation by oxidation of organic compounds
covalent chromatin modification
collagen fibril organization
Relative Proportion (%)
E
Hormone receptor correlations
AR
ESR1
Non−hormone
Both ER and AR
Female-specific
Male-specific
Non Sex-specific
Relative Proportion (%)
F
ESR1-driven
Female-specific
Non Sex-specific
Male-specific
G
ESR1-independent
Non Sex-specific
Male-specific
Female-specific
H
MSTN regulation
Hormone receptor correlations
F M
ESR1 4e-3 2e-3
AR 7e-4 4e-5
Bicor
-0.8 0 0.8
Human M/F
Fold change 6e-5
MERKO/WT
NS 4e-3
F M
Fold change
-3 1 3
MSTN immunoblot quantification
I
P=0.07
P=0.14
P=0.008
Relative intesity (MSTN/B-actin)
WT MERKO WT MERKO
Male
Female
J
Top male muscle MSTN pathways
carbohydrate catabolic process
cellular carbohydrate metabolic process
carbohydrate biosynthetic process
Relative enrichment ratio
K
Top female muscle MSTN pathways
respiratory electron transport
ATP synthesis
oxidative phosphorylation
Relative enrichment ratio

Figure 1: Figure supplement 1 - Skeletal muscle sex hormone receptor expression between sexes: Normalized gene expression levels for androgen receptor (*AR*) or estrogen receptor (*ESR1*) (y-axis) in each sex (x-axis). None of the expression levels were significantly different between sexes (students t-test,

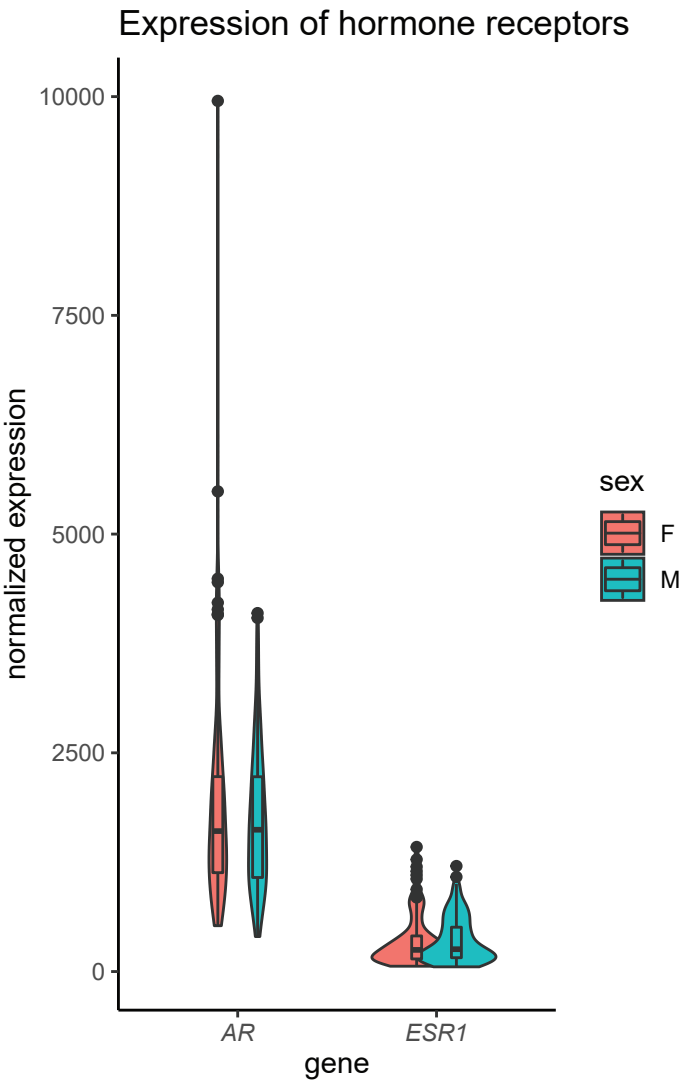

Figure 1: Figure Supplement 2 - Immunoblot for myostatin in EDL muscle from WT and MERKO male and female mice. Full Immunoblots shown for skeletal muscle lysate blotted for myostatin (top) or β-ac-tin (bottom) corresponding to different C57BL/6J male (left) or female (right) mice in either WT (floxed) or KO (floxed-cre) for skeletal muscle *Esr1*. Band sizes shown to indicate either precursor (top band) or processed/LAP form (bottom band) of myostatin.

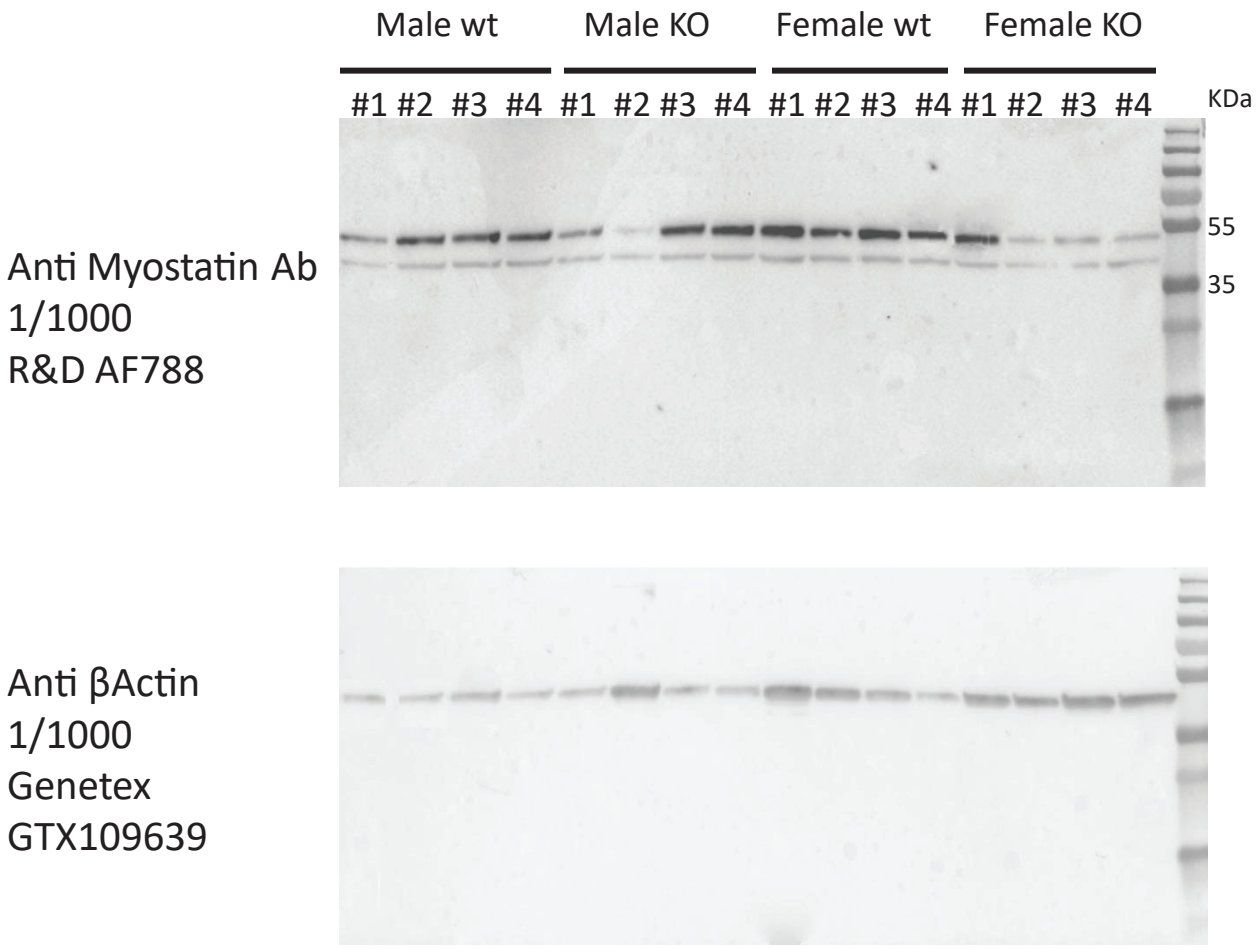

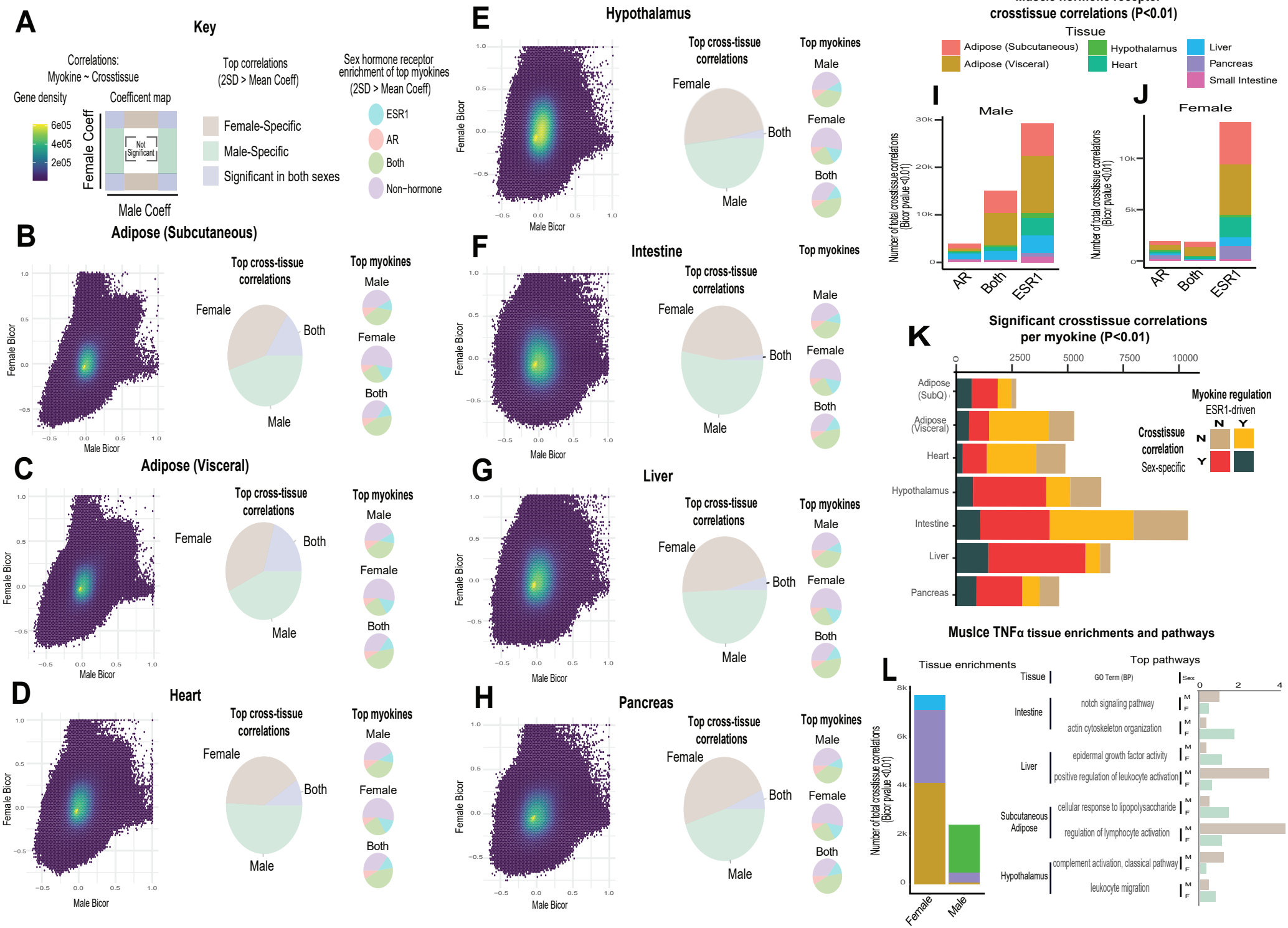
A
Key
Correlations:
Myokine ~ Crosstissue
Gene density
Coefficent map
6e05
4e05
2e05
Female Coeff
Not Significant
Male Coeff
Top correlations
(2SD > Mean Coeff)
Female-Specific
Male-Specific
Significant in both sexes
Sex hormone receptor
enrichment of top myokines
(2SD > Mean Coeff)
ESR1
AR
Both
Non-hormone
B
Adipose (Subcutaneous)
C
Adipose (Visceral)
D
Heart
E
Hypothalamus
F
Intestine
G
Liver
H
Pancreas
Female Bicor
Male Bicor
Top cross-tissue correlations
Female
Both
Male
Top myokines
Male
Female
Both
Muscle hormone receptor
crosstissue correlations (P<0.01)
Tissue
Adipose (Subcutaneous)
Adipose (Visceral)
Hypothalamus
Heart
Liver
Pancreas
Small Intestine
I
Male
J
Female
Number of total crosstissue correlations
(Bicor pvalue <0.01)
AR
Both
ESR1
K
Significant crosstissue correlations
per myokine (P<0.01)
Adipose (SubQ)
Adipose (Visceral)
Heart
Hypothalamus
Intestine
Liver
Pancreas
Myokine regulation
ESR1-driven
Crosstissue correlation
Sex-specific
N
Y
Musıce TNFα tissue enrichments and pathways
L
Tissue enrichments
Top pathways
GO Term (BP)
Sex
Tissue
Intestine
Liver
Subcutaneous Adipose
Hypothalamus
notch signaling pathway
actin cytoskeleton organization
epidermal growth factor activity
positive regulation of leukocyte activation
cellular response to lipopolysaccharide
regulation of lymphocyte activation
complement activation, classical pathway
leukocyte migration

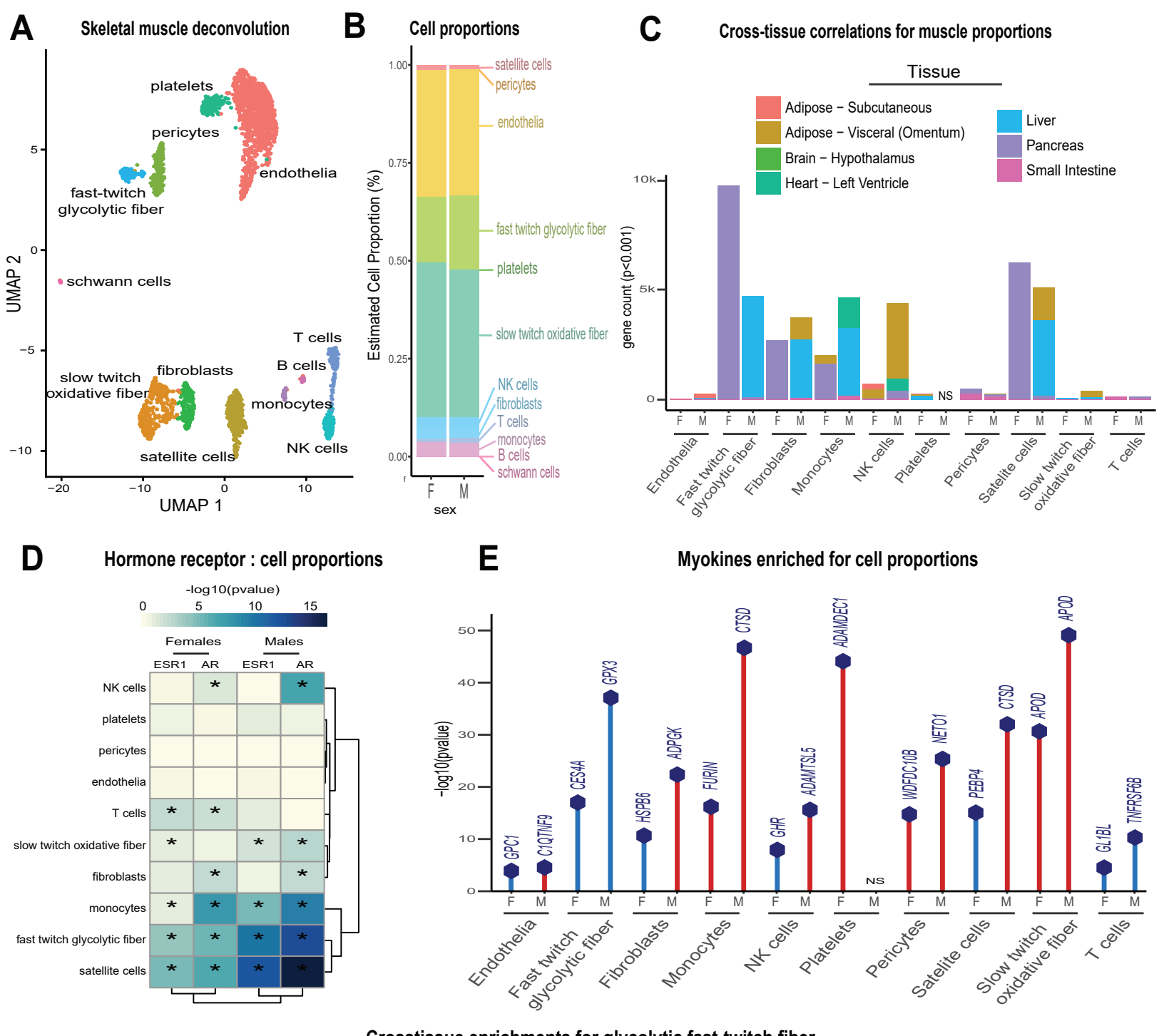
A
Skeletal muscle deconvolution
platelets
pericytes
endothelia
fast-twitch glycolytic fiber
schwann cells
T cells
B cells
fibroblasts
slow twitch oxidative fiber
monocytes
satellite cells
NK cells
UMAP 1
UMAP 2
B
Cell proportions
Estimated Cell Proportion (%)
sex
satellite cells
pericytes
endothelia
fast twitch glycolytic fiber
platelets
slow twitch oxidative fiber
NK cells
fibroblasts
T cells
monocytes
B cells
schwann cells
C
Cross-tissue correlations for muscle proportions
Tissue
Adipose − Subcutaneous
Adipose − Visceral (Omentum)
Brain − Hypothalamus
Heart − Left Ventricle
Liver
Pancreas
Small Intestine
gene count (p<0.001)
NS
Endothelia
Fast twitch glycolytic fiber
Fibroblasts
Monocytes
NK cells
Platelets
Pericytes
Satelite cells
Slow twitch oxidative fiber
T cells
D
Hormone receptor : cell proportions
-log10(pvalue)
Females
Males
ESR1
AR
NK cells
platelets
pericytes
endothelia
T cells
slow twitch oxidative fiber
fibroblasts
monocytes
fast twitch glycolytic fiber
satellite cells
E
Myokines enriched for cell proportions
-log10(pvalue)
GPC1
C1QTNF9
CES4A
GPX3
HSPB6
ADPGK
FURIN
CTSD
GHR
ADAMTSL5
ADAMDEC1
NS
WDFDC10B
NETO1
PEBP4
CTSD
APOD
APOD
GL1BL
TNFRSF6B
Endothelia
Fast twitch glycolytic fiber
Fibroblasts
Monocytes
NK cells
Platelets
Pericytes
Satelite cells
Slow twitch oxidative fiber
T cells
Crosstissue enrichments for glycolytic fast-twitch fiber
F
Top Pathways (p<1e-6)
protein targeting to ER
protein localization to endoplasmic reticulum
mRNA catabolic process
myeloid leukocyte activation
regulated exocytosis
Cell activation involved in immune response
Liver
Pancreas
Enrichment ratio
G
Crosstissue genes adjusted for myokine interactions
Liver inflammation and exocytosis
Pancreas protein synthesis
SAA1
VPS26A
EXOC3L1
CRP
STX11
TNFRSF1B
NFKB1
GRN
ALOX5
CD68
RPL14
RPL13A
RPL11
RPL10A
RPL10
Male
un-adj
GPX3 adj
Female
un-adj
CES4A adj
-log10(p)

Figure 3: Figure supplement 1- Comparisons of deconvolution methods Cell proportions were estimated from skeletal muscle sequencing across the 310 individuals in GTEx. Here, comparisons of the three most common methods (DCQ, NNLS and porportionsInAdmixture) were plotted for each pseudo-sc-proportion, where proportionsInAdmixture method captured the largest relative number of cell types

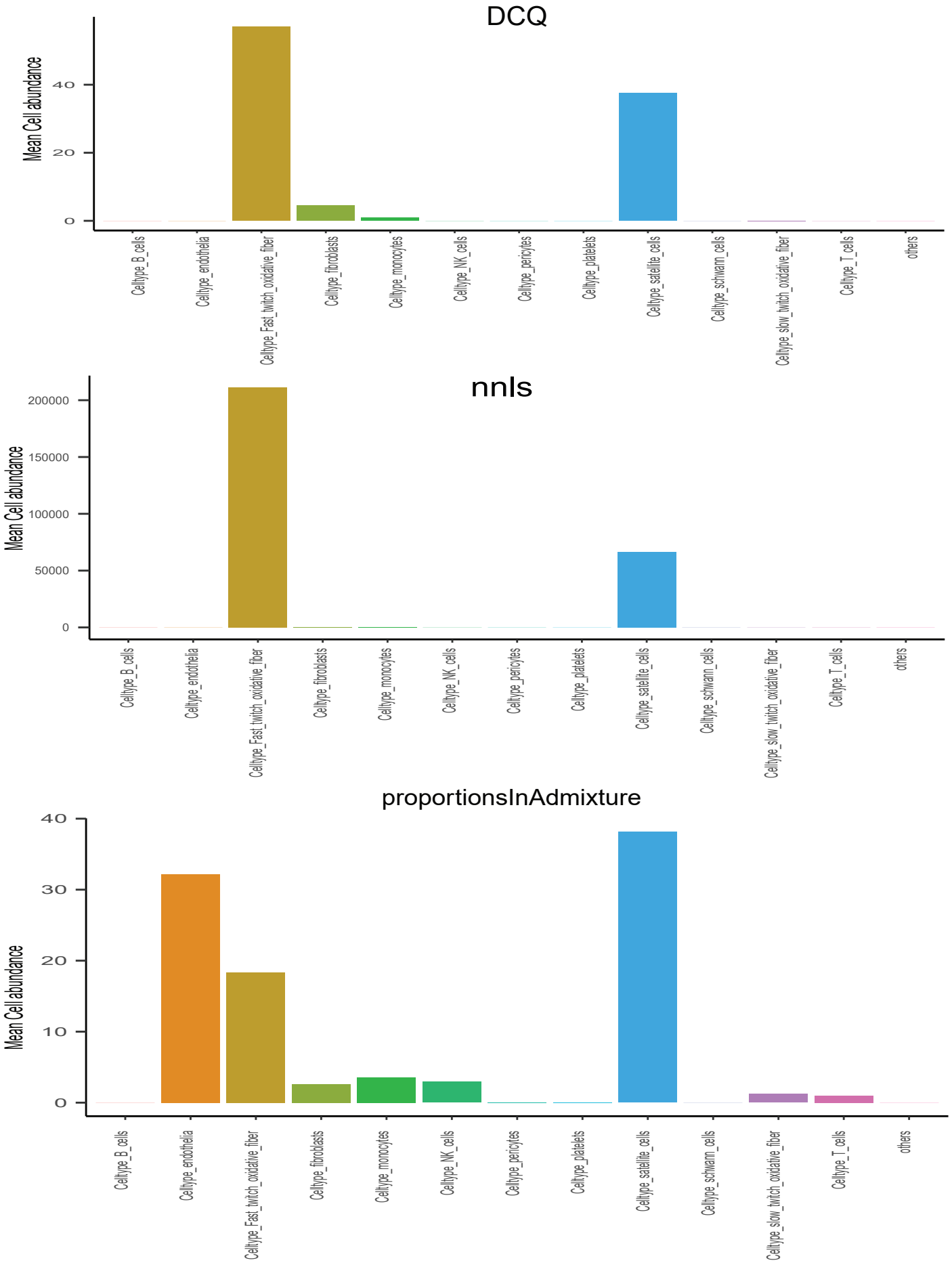

Figure 3: Figure supplement 2 - Cell composition correlations within each sex: Heatmaps showing regressions for cell proportions in males (left) or females (right), * = regression pvalue<0.01